INTERNATIONAL JOURNAL OF INNOVATIVE RESEARCH IN MULTIDISCIPLINARY EDUCATION

ISSN(print): 2833-4515, ISSN(online): 2833-453

Volume 03 Issue 06 June 2024

DOI: 10.58806/ijirme.2024.v3i6n28, Impact factor- 5.138

Page No. 1121 - 1136

Smart Nanocomposite in the SiC-Si-Al-Al_2O_3-Geopolymer System

Zviad. Kovziridze[1], Natela. Nijaradze[2], Gulnaz. Tabatadze[3], Temur. Cheishvili[4], Maia. Mshvildadze[5], Marina kapanadze[6], Maia Balakhashvili[7], Nino Daraxvelidze[8]

[1,2,3,4,5,6,7,8] Georgian Technical University, Institute of Bionanoceramic and Nanocomposite Technology Bionanoceramic and Nanocomposite Materials Science Center. ,69, Kostava Str., Tbilisi 0175, Georgia

ABSTRACT: Goal-obtaining of composite in the SiC-Si-Al-$Al_2O_{3\ (nanopowder)}$-geopolymer system with the metal-thermal method in the nitrogen medium. **Method**- In the present paper nanocomposite with SiALON was obtained through alum-thermal process in the nitrogen medium on the base of Geopolymer (kaolin and pology cley – Ukraine), SiC, alumina oxide nanopowder, aluminum nanopowder and Si powder with small additives of glas perlite (Aragatz, Armenia) by the reactive baking method. The advantage of this method is that compounds, which are newly formed thanks to interaction going on at thermal treatment: Si_3N_4, Si, AlN are active, which contributes to SiALON formation at relatively low temperature, at 1250-1300^{0}C. **Results**-ß-SiAlON was formed at the sintering of SiC-aluminium and silicium powder, geopolymer at 1450^{0}C. Porosity of carbide SiAlON composite obtained by reactive sintering, according to water absorption, equals to 13-15%. The samples were fragmented in a jaw-crusher and were powdered in attrition mill till micro-powder dispersion was obtained. Then samples were hot-pressed at 1620^{0}C under 30 MPa pressure. Hold-time at the final temperature was 8 min. Sample water absorption, according to porosity, was less than 0.4%. Further studies were continued on these samples. **Conclusion-t**he paper offers processes of formation of SiC-SiAlON composites and their physical and technical properties. Phase composition of the composites was studied by X-ray diffraction method, while the structure was studied by the use of optic and electron microscope.

Electric properties showed that the specimen A obtained by hot-compression is characterized by 2 signs lower resistance than the porous material B, which was used to receive this specimen. Probably this should be connected with transition of the reactively baked structure of the hot-compressed material into compact structure. Obtained materials are used in protecting jackets of thermo couples used for melted metal temperature measuring (18-20 measuring) and for constructions used for placing objects in factory furnaces.

KEYWORDS: alum-thermal process, nitrogen medium, SiAlON, SiC, Al_2O_3, composite.

1. INTRODUCTION.

Ceramic that contains various phases in the system Si-Al-O-N is called SiAlON. SiAlONs belong to the simonyite class [1]. Structural unit of SiAlONs is a tetrahedron (Si, Al) $(ON)_4$ similar to tetrahedron SiN_4 in silicon nitride and silicon oxynitride-SN_2O. SiAlONs contain the structural types and phases, which are based on: aluminum nitride, apatites, silicon α and ß nitride, silicon oxynitride, spinels and others. SiAlON-s can be obtained in neutral atmosphere at 1600^{0}C, by reactive sintering at 2000^{0}C or by hot-compression at 1750^{0}C or higher temperatures in the mixes: aluminum nitride and silicon, aluminum oxide and silicon oxide, silicon oxynitride as well as by lithium-aluminum or magnesium-aluminum spinels. Single phase SiAlONs can exist in relatively narrow region with the formula $Si_{(6-X)}Al_XO_XN_{(8-X)}$ where X varies from 0 to 5. In the system of SiAlONs the $Si_3Al_3O_3N_5$, which is structurally close to silicon nitride and by its chemical properties close to aluminum oxide has been studied better than other SiAlONs.

There are several types of SiAlONs: α; β; X; O^1; H; R [2-6]. These types can be used as construction materials in the medium oxidizing up to 1300^{0}C and in the medium non-oxidizing up to 1800 ^{o}C. [6-8].

Table 1 offers chemical compositions and structural types of SiAlONs. The system Si-Al-O-N can be described as a four-component one and schematically can be imagined as a tetrahedron, with the component elements in its nodes (Fig.1). Double compounds are spread on tetrahedron edges; up to 1800^0 they preserve normal valence. Besides, all possible combinations which contain four

Table 1. Names and structures of SiAlONs phases

name	chemical formula	structure type
α	$Me_x (SiAl)_{12} (ON)_{16}$ X=0÷2	α-Si_3N_4
β	$Si_{6-X} Al_x N_{8-X}$ X=0 ÷ 4.2	β-Si_3N_4
O^1	$Si_{2-X} Al_X O_{1+X} N_{2-X}$ X=0.04÷ 0.4	Si_2ON_2
X	$Si_{2-X} Al_{1-X} O_x N_{1-X}$ x= 0.04 ÷ 0.2	$3Al_2O_3$• $2SiO_2$
H	$SiAl_3O_2N_3$ $SiAl_5O_2N_5$	AlN
R	$SiAl_4O_2N_4$ $SiAl_6O_2N_6$	AlN

2.Major part

Table 2 offers material composition of the studied object.

Table 2 CN-21 composite material composition, mass%

Name	geopolymer-kaoline Prosiannaia (Ukraine)	geopolymer-Pology clay fire proof (Ukraine)	Al_2O_3	SiC	Si	Al	Perlite (Armenia)	MgO	Y_2O_3
CN-21	13.9	4.6	18.2	23.8	22.0	12.0	2.8	0.9	1.8

elements are spread in the plane - Si_3N_4- -SiO_2-Al_2O_3-AlN, it can be divided into two isosceles triangles, which are triple systems Si_3N_4-Al_2O_3-SiO_2 and Si_3N_4- Al_2O_3-AlN [9-13].

Pology clay chemical composition (mass%): SiO_2-47.92, Al_2O_3-35.20, Fe_2O_3-2.06, CaO-0.40, MgO-0.30, K_2O-2.00, Na_2O-0.50, loss at heating-12.24; fire-resistance 1710-1730^{0}C.

Chemical composition of kaoline (mass%): SiO_2-46.45, TiO_2-O.33, Al_2O_3-38.70, Fe_2O_3-0.46, MgO-trace, CaO-0.36, Na_2O-0.45, K_2O-0.60, loss at heating 13.63.; fire-resistance-1770^{0}C. Fig 2 offers phase equilibrium graph, where phases are considered SiAlONs. Single phase area (β^1- SiAlONs) is spread along X composition (Al_2O_3·AlN)+(1-X) Si_3N_4, where X=0÷0.8, but the lines with the cation/anion ratio=3/4. Creation of solid liquid of Al_2O_3 -and AlN-in β-Si_3N_4- doesn't need the presence of

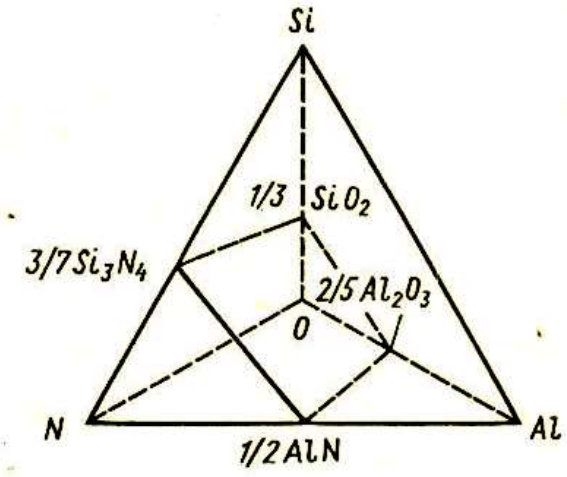

Fig.1. Scheme of distribution of components in Si-Al-O-N system.

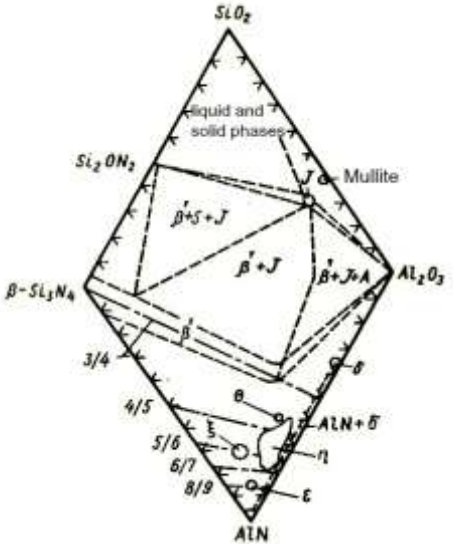

Fig. 2. Si_3N_4-AlN -Al_2O_3-SiO_2 system phase graph.

vacancies of inculcated cations and anions in crystalline lattice of β-Si_3N_4. At the increase of Al^{3+} and O^{2-}concentrations we observe linear growth of β-Si_3N_4 – lattice in solid liquid [14-21]. Optimal phase composition of cutting instrumental SiAlONs is: 75% SiAlON and 25% glassy phase. We added glassy perlite of Aragats (Armenia) to the mix, up to 3 mass%. Glassy perlite consisted of 96% glassy phase and the rest are structural water and gasses. Perlite undergoes dehydration at 860^0C; the structure becomes friable which contributes to intensification of diffusion processes and to the creation of conditions for creation of new phases. Fig. 3 offers perlite thermogram, while Fig. 4 – X-ray diffraction patterns of raw perlite and perlite sintered at 900 ° C; these patterns prove that it is completely a glassy phase. Chemical composition of perlite (mass %) is as follows: SiO_2-73.48, Al_2O_3-14.03, Fe_2O_3-0.62, CaO-0.60, MgO-0.47, SO_3-0.25, R_2O-6.50, loss at heating-3.42. [22].

Fig.3 Perlite thermogram

Fig.4 Perlite X-ray diffraction patterns. a) Upper –raw perlite; b) lower – perlite sintered at 900^0C

According to the X-Ray diffraction pattern of CH-7 that was obtained by reactive sintering at 1450^0C (Fig.5) by the use of by metalothermal and nitriding method, the main phase is ß – SiAlON. The composite, alongside with ß– SiAlON contains X-SiAlON, in insignificant amount. In the CH 7 composite matrix we observe carbide grains, which by their size exceed that of the just-formed silicon nitride grains [23].

The data of micro-structural study of CH 21 composite (Fig.6) are in conformity with the results of X-ray structural analysis, which shows that the matrix of this composite is ß- SiAlON.

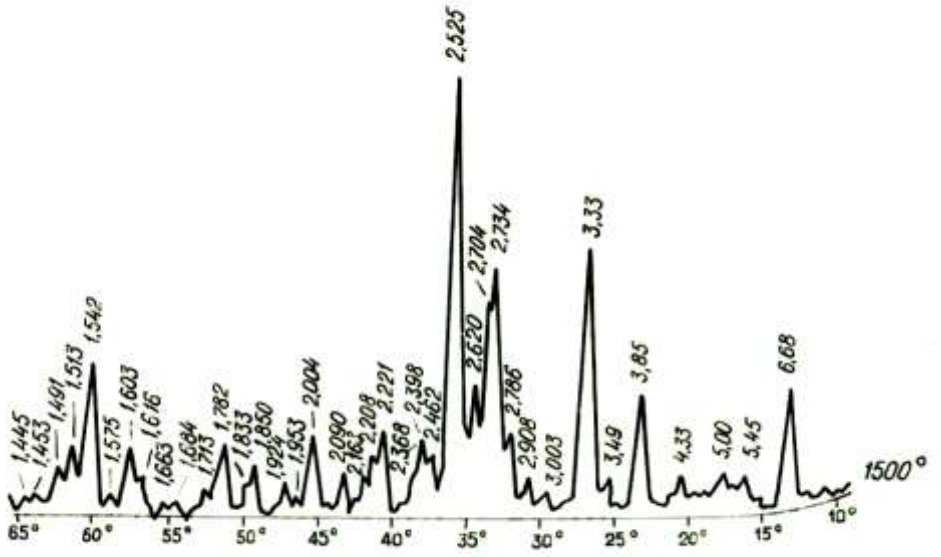

Fig. 5. X-Ray of CH-21 composite sintered by reactive method (1450^0C)

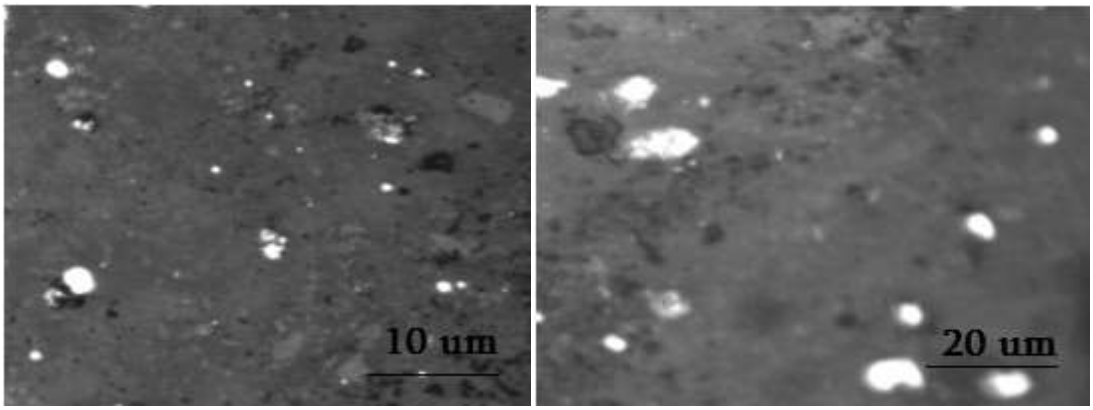

CH-21 X-200 CH-21 X-500

Fig. 6 CH-21 composite optical-microscopy morphology

Materials selected for obtaining composites: kaoline, Pology clay, aluminum nano-powder, SiC, Si, perlite, and additives:Y_2O_3, MgO, after weighing (batching) were grinded in porcelain ball- mill. To receive the mold the mix was pressed under hydraulic press at 20 MPa. The molded specimens were dried on air for 24 hr and then in a drier at 110^0C. It was sintered in silite furnace in nitrogen medium at $1400\text{-}1500^0$C; hold-time at final temperature was 30 min. Ready product, after furnace cutoff was cooled together with a furnace in free regime.

To receive a hard product the composite CH-21 obtained by reactive sintering and nitro-alumino-therman methods was fragmented in a jaw crusher, grinded in a ball-mill for 8 hours and then in an attritor mill – for 8-10 minutes.

At hot compression, at low temperature, active process of crystallization, that is, growth of sintered substances doesn't start yet. This means that the sintered product will have fine-grain structure and high specific density.

Precursor for hot compression was prepared in a thermostat at 150^0C, it was cold-pressed twice under 12-15MPa and 20-25 MPa; was hot-compressed at 1620^0C under 30 MPa, vacuum equaled to 10^{-3} Pa, hold-time at final temperature 10-12 min; sintering regime was as follows: $20\text{-}500^0$C 7^0C /min, $500\text{-}1400^0$C- 150 ^{0}C/min, 1400-1620 ^{0}C 10 ^{0}C/min.; cooling 10 ^{0}C/min. Temperature regime of sintering is given on Fig. 7.

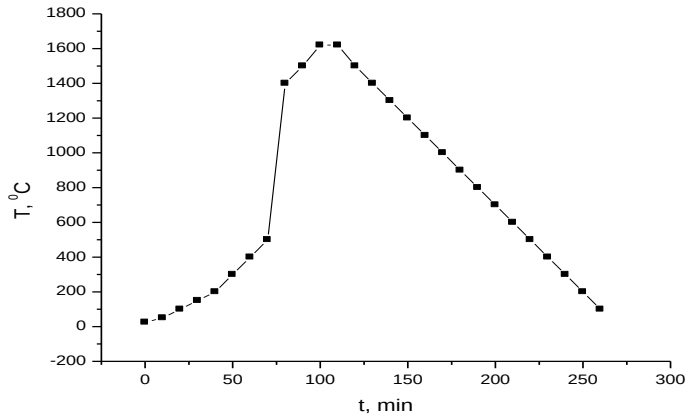

Fig. 7. Temperature regime of hot-compression sintering of CN-21 at 1620^{0}C

We investigated physical-technical characteristics of a sample that was hot-compacted at 1620^{0}C. The obtained results are given in Table 3. Water absorption value of hot-compressed sample according to porosity is less than 0.3%, while the ultimate strength at compaction 1910 MPa. hardness = HV-19.70. The data given by us in the table enable us to conclude that 1620^{0}C is a sufficient temperature for complete hardening of specimens.

Table3. Physical-technical characteristics of hot-compressed CH-21 sample

composite index	open porosity **w,%**	general porosity**, P, %**	density**, ρ, g/cm^3**	**compression pressure,** MPa.	ultimate compressive strength**, σc,** MPa.	ultimate bending strength**, σb,** MPa.
CH-21 (1600^0)	0.28	3.10	3.17	30	1910	470

Table 4.Mechanical characteristics of hot-compressed CH-7 sample

composite index	**Kic,** MPa.	**fragmentation factor, B,** MPa.	**n –factor**
CH-21 (1620^0)	5.54	4.56	-2.44

The value of computed fragmentation factor of the material is given in Table 4.

Quantitative factor of fragmentation (B) was determined which was obtained on the basis of the value of experimentally defined micro-hardness and tension intensity critical coefficient (Kic):B=Hv/Kic. Low value of fragmentation implies low chances of catastrophic spread of cracks [24].

According to Anstis [25] $Kic=0.0016\ P/C_0^{3/2}\ (E/H)^{1/2}$ GPa. where P is for loading in Newton-N; Co-crack length from the indentation center to the crack top in meters; E-Young's modul in GPa; V-micro-hardness according to Vickers, in-GPa.

n-factor is an important parameter at mechanical processing of materials. This factor enables us to speak of easiness of machine processing of the material. n=0,643-0,122 Hv; ceramic and ceramic composite will be processed easily if it has positive n-value [24]. In case of our material, cutting as well as mechanical processing for grinding is complex due to high hardness of material. It should be stated that while cutting by diamond abrasive discs we encountered resistance, which damaged some diamond grinders and this, quite naturally contributed to developing cracks in the material. It decreased mechanical properties of our material. It would be better to have the possibility to process by laser cutting. Dynamic micro-hardness and elasticity modulus of the obtained materials were determined according to the demands of International standard ISO-14577 by the dynamic ultra-

micro-hardness tester DUH 211S, which is used for determination of mechanical characteristics (micro-hardness, elasticity module) of solid bodies. Results are given in Table 5. .

CN-21 composite technical characteristics Table 5. <<Test condition-SiAlON-200 >>

Test mode	Load-unload		
Sample name	SiAlON-zv	Sample No.	#1
Test force	200.000[gf]	Minimum force	0.200[gf]
Loading speed	1.0(7.1448[gf/sec])	Hold time at load	5[sec]
Hold time at unload	3[sec]	Test count	21
Parameter name	Temp	Parameter	20
Comment	21.06.17-SiAlon-zv-200;DHV5-3		
Poisson's ratio	0.190		
Cf-Ap,As Correction	ON	Indenter type	Vickers
Read times	2	Objective lens	50
Indenter elastic	1.140e+006[N/mm2]	Indenter Poisson's ratio	0.070

< Test result >

SEQ	Fmax	hmax	hp	hr	DHV-1	DHV-2	Eit	Length	HV	Data name
	[gf]	[um]	[um]	[um]			[N/mm2]	[um]		
1	200.710	4.7107	1.9264	3.1017	442.157	2643.803	7.211e+004	15.792	1492.537	SiAlON-200(2)
2	200.786	4.2612	1.6795	2.7414	540.546	3479.868	8.707e+004	14.621	1741.886	SiAlON-200(4)
3	200.800	4.9636	1.7638	3.3296	398.419	3155.263	6.588e+004	16.959	1294.659	SiAlON-200(5)
4	200.674	4.5307	1.7788	3.0421	477.884	3100.234	8.083e+004	15.644	1520.484	SiAlON-200(6)
5	200.675	4.3294	2.1587	2.9575	523.381	2105.199	9.024e+004	15.498	1549.415	SiAlON-200(7)
6	200.662	3.5295	1.5855	2.1773	787.444	3902.198	1.254e+005	16.595	1351.275	SiAlON-200(8)
7	200.661	3.6147	1.8441	2.4494	750.723	2884.448	1.349e+005	17.179	1260.907	SiAlON-200(9)
8	200.738	3.0333	1.1085	1.7530	1066.516	7985.353	1.660e+005	12.866	2248.651	SiAlON-200(10)
9	200.959	2.8595	1.0929	1.5884	1201.396	8224.728	1.857e+005	12.134	2531.125	SiAlON-200(11)
10	200.866	3.0653	1.3375	2.0446	1045.024	5488.768	1.924e+005	-----	-----	SiAlON-200(12)
11	200.737	3.1154	1.3372	2.0317	1011.028	5488.160	1.790e+005	-----	-----	SiAlON-200(13)
12	200.960	2.5787	1.1425	1.5447	1477.302	7525.888	2.536e+005	12.135	2530.738	SiAlON-200(14)
13	200.923	2.7215	1.1113	1.5055	1326.134	7952.513	2.077e+005	11.989	2592.358	SiAlON-200(16)
14	200.501	2.8549	1.0966	1.5509	1202.544	8150.998	1.824e+005	12.135	2524.953	SiAlON-200(17)
15	200.497	3.4966	1.3136	2.2145	801.640	5679.626	1.320e+005	-----	-----	SiAlON-200(18)
16	200.702	2.9626	1.1801	1.6771	1117.798	7044.719	1.729e+005	12.428	2409.746	SiAlON-200(19)
17	200.589	3.4541	1.4444	2.0858	821.888	4700.234	1.288e+005	14.474	1775.634	SiAlON-200(20)
18	201.195	3.0666	1.0307	1.5932	1045.886	9257.288	1.515e+005	11.698	2726.384	SiAlON-200(21)
Average	200.757	3.5082	1.4407	2.1882	890.984	5487.183	1.449e+005	14.143	1970.050	
Std. Dev.	0.174	0.738	0.346	0.611	324.195	2330.548	52250.109	2.028	548.126	
CV	0.087	21.043	23.994	27.907	36.386	42.473	36.057	14.341	27.823	

Fig 8 offers composite's micro-mechanical characteristics

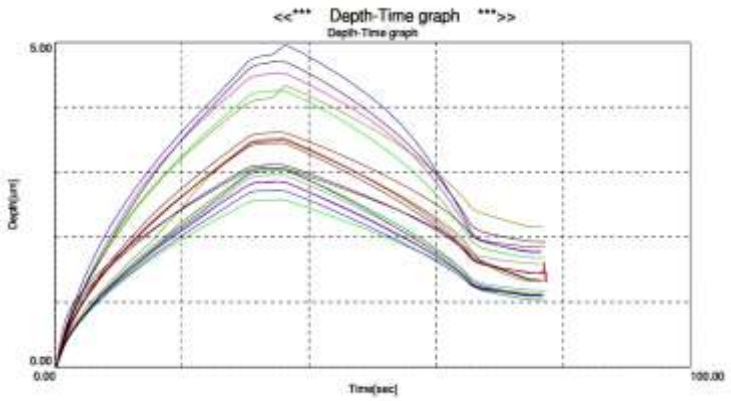

a)

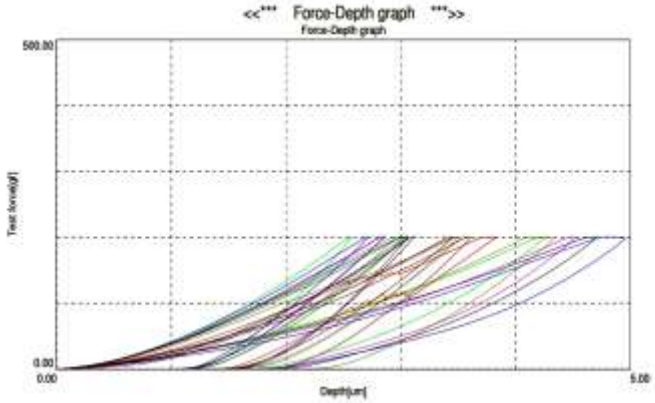

b)

Fig. 8. CN-21 composite micro-mechanical characteristics at 2N load a) indenter depth-time dependence ; b) indenter load-indentation depth dependence .

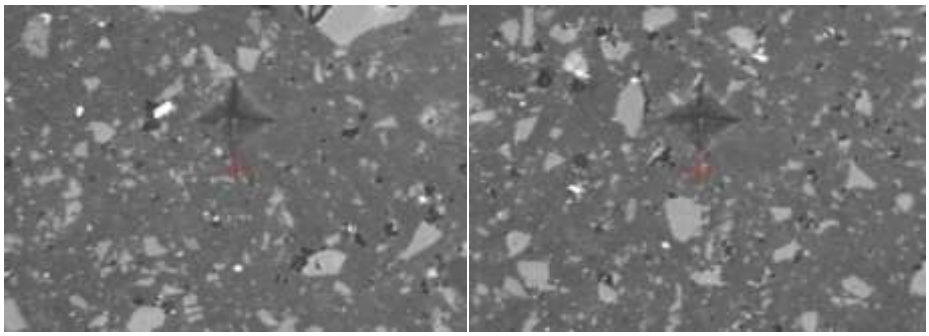

a) **b)**

Images of indentations in matrix, at the interface of matrix and grains and on grains are given in Figures 9,10,11.

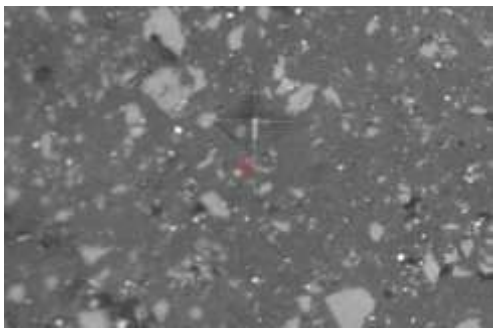

c)

Fig. 9 a), b), c) indentations in matrix

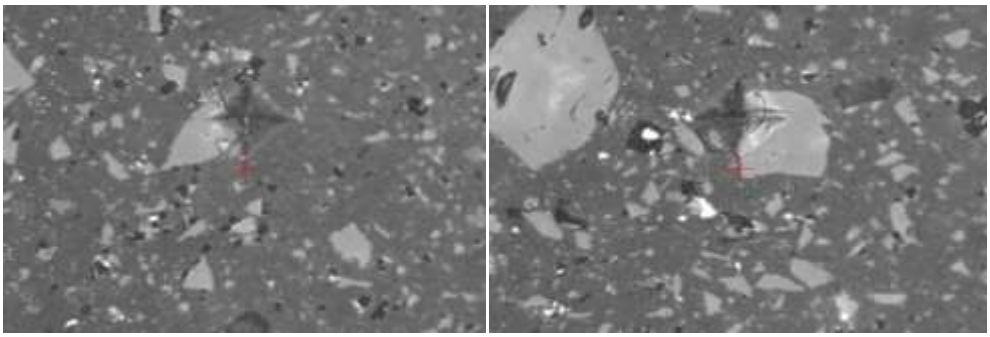

a) b)

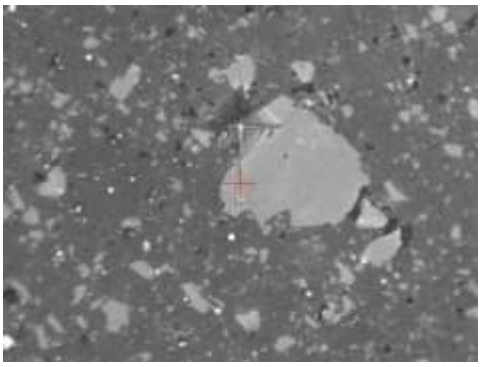

c)

Fig. 10. a), b), c) Indentation on the border of silicon carbide and matrix

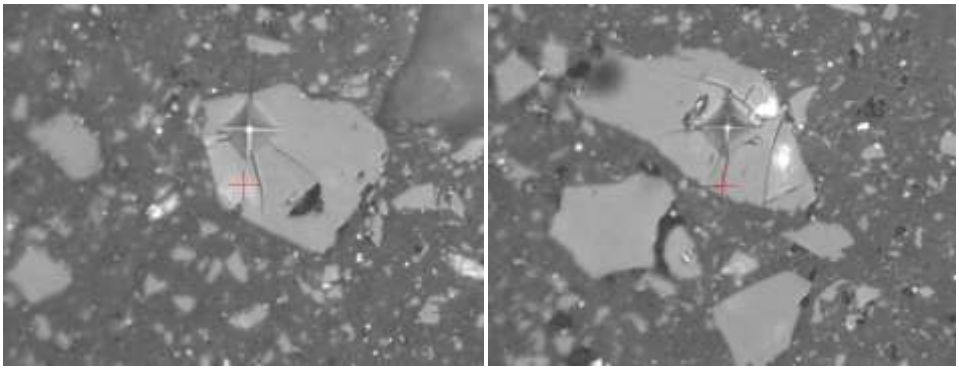

a) b)

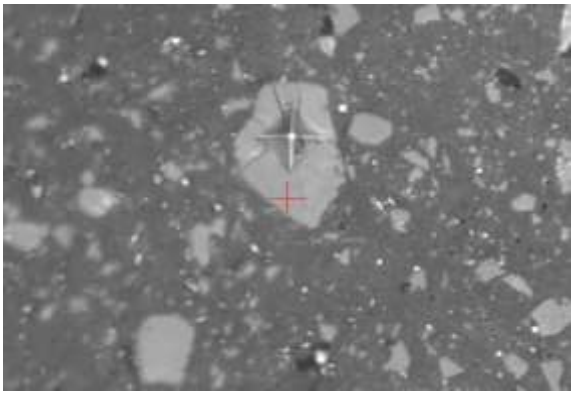

c)

Fig. 11 a), b), c) indentations on the silicon carbide grain

Fig. 8, 9,10 and 11 should be considered in one context.

Results are offered in Table 5. Table 5 gives the results of tests carried out on the CH-21 specimen hot-compacted at 1620^0C, indentation reading is taken from matrix (Fig.9); indentation readings were taken several times and results are given in the Table according to which average hardness is HV: 19,70GPa. Dynamic hardness DH-8.9 GPa, elasticity module E-145 MPa.

Indentations on SiAlON matrix given on Fig.9 shows that indentation form is sharp, with clearly cut edges. We don't see a crack along the edges on the Fig. 9 a). On Fig. 9 b) we observe a small, 6.6 μM size crack along the right edge of the indentation, while on Fig. 9c) we again observe a small 7.0 μM size crack along the right edge of the indentation, which speaks of homogeneity of SiAlON matrix and of its high relative density.

Indentation readings taken on the border of a matrix and grain are rather interesting. Length of indent diagonal on the Fig 10 a) is 17 μM. Average crack length on the grain is- 5.75 μM. Crack spreading in matrix is not observed. Indentation diagonal length on Fig.10 b) is 12 μM., while average length of a crack on the grain is 5.22 μM. Crack development in the matrix is not observed. Grain has just one crack. Fig.10 c) shows that indentation length is 12 μM, while average length of a crack-11.71 μM..

Table 5 offers test results of SiC grains of the composite CN-21 microstructure. Indentation was made at 2 N loading on SiC grains.

Borders of indentations on carbide grains are sharp (Fig. 11 a), b) c)); a crack which is formed at the indenter load on the grain doesn't spread beyond the grain limit. Matrix, because of its high mechanical properties and energy dissipation, subdues crack spreading and the composite strength is preserved. Such big size grains are rare (Table 8) and discussion about material mechanical properties should not be relevant, since increase of their dispersion grade is not a problem, while it gives interesting picture for the research of the issue. Especially interesting is a Figure 11 b). In this case a crack on the right side of the indentation is developing so intensely that it reaches matrix and colliding with the strong matrix, goes back, transects the grain diagonally and collides with the matrix from the other side of a grain, but fails to destruct it. It should be stated that the crack keeps its high energy and develops diagonally on the other side of SiC grain, but having lost its energy is unable to reach matrix. Crack which spreads from the lower edge reaches matrix, but energy dissipation in a grain and matrix Kic is so high, that a crack disappears at the matrix. Fig.11 a) and c) show clearly directions of crack development. As is known in this instance Kic is most important for material crack-resistance, since a crack, after it is detached, is developed by 2000 m/sec speed and at this time material resistance is determined not only by the speed of crack shock on matrix, but also by Kic value.

Dynamic micro-hardness (DH) is determined by indenter load value and depth of indentation in the material in the process of testing. Its significance is computed by the formula: $DH=a \times F/h^2$; where "a" is a constant value and depends on indenter form; for Vicker's indenter it equals to a=3.8584.

Advantage of the method over the common, static method, that is, measuring of linear sizes of an indentation (diagonal) is that it contains plastic as well as elastic components. Results of measuring don't depend on indentation sizes, loads and non-homogeneity of elastic restoration.

Dynamic hardness was determined in load-unload regime, till elastic relaxation started, by taking seven readings per each concrete load tested, by discarding two extreme values and by averaging the remaining five values. The value of micro-hardness was determined mechanically. Hold time at maximum load equaled to 5 sec, at the end of unload – 3 sec (Fig. 8 a) b).

Indentation was made in the matrix of a specimen consisting of β- SiAlON. As a result of testing its mean hardness equaled to DHV=8,9 GPa which is a rather high value.

From the load-unload relation diagram (Fig. 8) we define the value of elasticity module by determination of hardness $S=(dF/dh)\ h\text{-}h_{max.}$- .It is a tangent of load-unload diagram at the starting point of unload. A device defines elasticity module of the material under the study and its mean value in case of our material E=145 GPa. (Fig.5). Indentation pictures are in full conformity with graphical data on Fig. 8. As is seen from Fig.8 a) indentation reading taking lasted 78 seconds and 18 indentation readings were taken. Depth of every indentation varies and it varies from 2.5 to 55 μM. As we see 2N load is somewhat high than optimal load for this material. The same is evidenced at the application of test force (200 g approximately =2N) when we define indentation depth (Fig. 8 b)). In this case, again indentation depths for all 18 tests vary and they vary from 2.5- to 5 μM. For comparison we take Table 6 and Fig. 12, which show that all indentations in SiALON matrix are almost of the same depth at 1N load (100 g). We can conclude that optimal load for such composition material is 1N.

Table 6. CN-21 composite technical characteristics at 1N load < Test condition-SiAlON-100 >

Test mode	Load-unload		
Sample name	SiAlON-zv	Sample No.	#1
Test force	100.000[gf]	Minimum force	0.200[gf]
Loading speed	1.0(7.1448[gf/sec])	Hold time at load	5[sec]
Hold time at unload	3[sec]	Test count	23

Parameter name	Temp	Parameter	20
Comment	20.06.17-SiAlON-zv-100;DHV5-3		
Poisson's ratio	0.190		
Cf-Ap,As Correction	ON	Indenter type	Vickers
Read times	2	Objective lens	50
Indenter elastic	1.140e+006[N/mm2]	Indenter Poisson's ratio	0.070

< Test result>

SEQ	Fmax	hmax	hp	hr	DHV-1	DHV-2	Eit	Length	HV	Data name
	[gf]	[um]	[um]	[um]			[N/mm2]	[um]		
1	100.753	2.0927	1.0353	1.3623	1124.606	4595.143	2.023e+005	12.133	1269.108	SiAlON-100(1)
2	100.862	2.1408	1.1973	1.4454	1075.849	3439.729	2.028e+005	10.673	1641.878	SiAlON-100(2)
3	100.954	2.1185	1.0085	1.3472	1099.608	4852.203	1.911e+005	11.989	1302.427	SiAlON-100(3)
4	100.844	2.1300	0.9980	1.3526	1086.598	4949.256	1.881e+005	11.623	1384.295	SiAlON-100(4)
5	100.935	2.1822	1.1183	1.4290	1036.181	3945.265	1.855e+005	12.721	1156.721	SiAlON-100(5)
6	100.624	2.0945	1.0240	1.3135	1121.301	4691.482	1.921e+005	11.843	1330.428	SiAlON-100(6)
7	100.551	2.1229	1.0193	1.3350	1090.715	4731.042	1.868e+005	11.551	1397.624	SiAlON-100(7)
8	100.826	2.1357	1.0016	1.3362	1080.626	4912.610	1.834e+005	11.550	1401.679	SiAlON-100(8)
9	100.826	2.1173	0.9846	1.2881	1099.473	5084.458	1.815e+005	11.404	1437.730	SiAlON-100(9)
10	100.825	2.1761	1.0974	1.4160	1040.858	4092.733	1.848e+005	11.697	1366.620	SiAlON-100(10)
11	100.807	2.1566	1.0491	1.3859	1059.580	4477.130	1.857e+005	-----	-----	SiAlON-100(11)
Average	100.801	2.1334	1.0485	1.3646	1083.218	4524.641	1.895e+005	11.718	1368.851	
Std. Dev	0.120	0.029	0.064	0.049	28.966	502.835	7155.469	0.529	125.730	
CV	0.119	1.372	6.141	3.617	2.674	11.113	3.777	4.518	9.185	

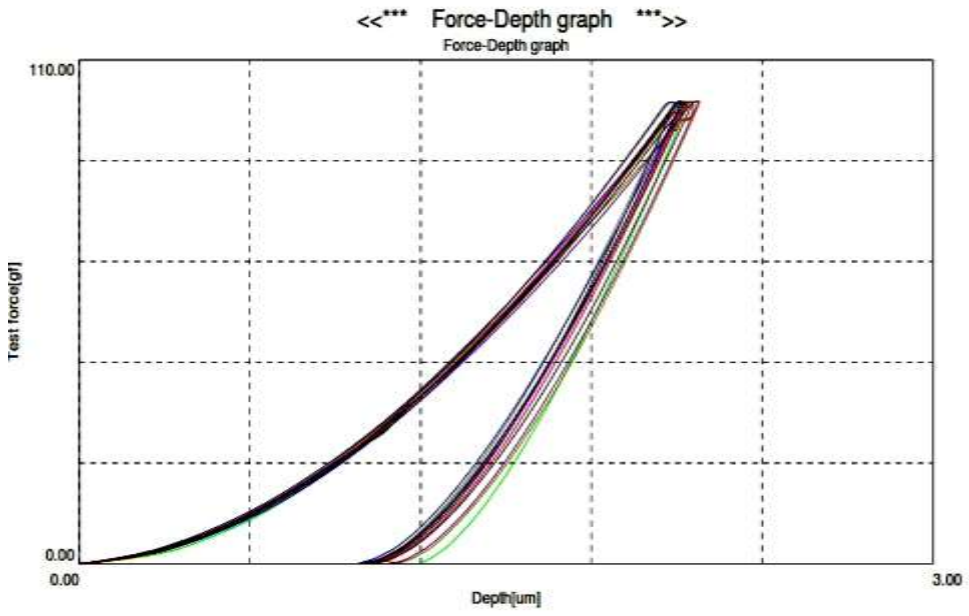

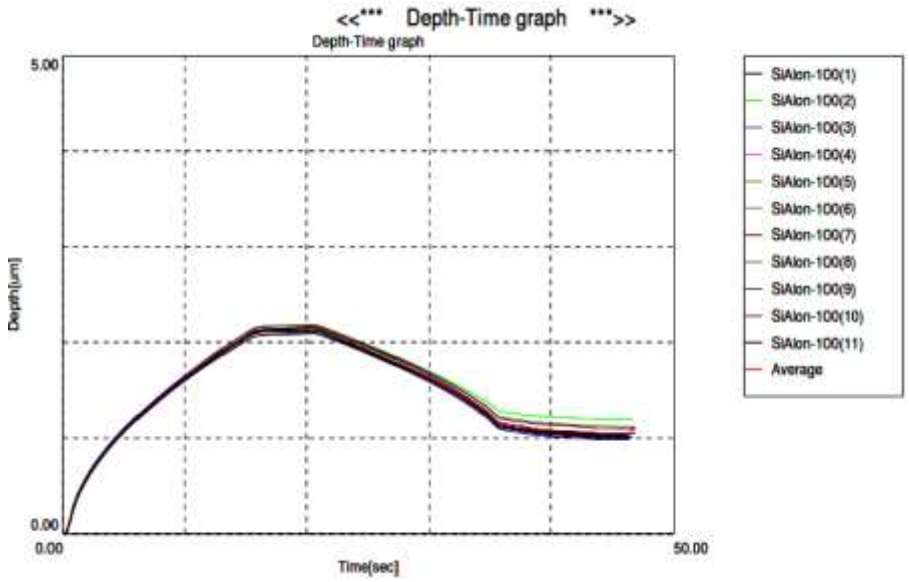

Fig. 12 CN-21 composite micromechanical characteristics at 1 N load a) indentation depth-time relation; b) indentation load - depth relation

Table 7 Average sizes of indentations and cracks

indentation picture №	indentation diagonal length, a, µM	half indentation diagonal a/2. µM	crack mean length ℓ, µM	sizes of SiC grain with indentations, µM	note
14	12.135	6.067	10.40	A-50.8 B-28.8	indentation on the referred size grain
16	12.428	6.214	10.40	A-54,8 B-25.6	-„-
17	14.474	7.237	8.20	A-33.3 B-20.8	-„-
average			9.67		
3	16.959	8.479	5.75	A-17.24 B-10.34	indentation on the interface of the referred size grain and matrix
12	12.135	6.067	5.22	A-17.24 B-17.24	-„-
13	11.989	5.994	11.71	A-20.64 B-27.59	-„-
average			7,56		
2	14.621	7.310	cracks are not fixed		indentation on matrix
4	15.644	7.822	7.00		-„-
7	17.179	8.589	6.80		-„-
average			4.50		

In this case, hardness according to Vickers equals to 13.68 GPa. Average indentation depth -2.13 μM; dynamic hardness DHV= 10.83 GPa. E=189 MPa . Indentation diagonal -11.71 μM. The table and graphical material shows that SiAlON matrix is homogeneous and its properties, irrespective of readings taken from various spots of matrix, are not characterized by fluctuation

(Table 7). Mechanical module of materials To compute mechanical module of material we used Kovziridze's module [26-27]:

$$M=\frac{Kvol.E.Kic.P_d}{Km.Gvol..Pvol..Pm}\ MPa/\ \mu M^2.$$

where, Kvol. is crystalline phase volume in the material, in %; E –elasticity module-MPa; Kic- critical stress intensity coefficient; P_d –pore dislocation factor in matrix, which was considered equal to 1 in case of homogeneous redistribution, 0.9 – in case of non-homogeneous redistribution and 0.8-in case of pores coalescence. Km –average size of crystals in matrix - μM ; Gvol-glassy phase composition in matrix, in %; Pvol.-volume of pores in matrix – in %; Pm-average pore size in matrix-μM . Module dimension MPa/ μM^2. The formula doesn't consider Griffith's [28] cracks, dislocations in crystals, nano-defects in glass, but the formula gives us thorough impression about resistance of materials to external loads, which is approximated to the values computed for strength of bonds between atoms. This is namely why the elasticity module was inserted in the formula.

Electron-microscopy(Fig.13-14) and X-Ray structural analyses(Fig.15) were performed for phase analysis, while for computation of Kic, micro-mechanical properties were investigated, the results of which are considered above. Investigation of structural-morphological and element composition of specimens was performed by scanning electron-microscope JSM-6510LV of Japanese company JEOL, which is equipped with energy dispersion micro-rentgeno spectral analyser X-Max^N-of the British company OXFORD INSTRUMENTS. Electronic surface images were obtained in the secondary (SEI) as well as in reflected (BES) electrons by the use of 20 kW accelerating voltage. In some cases, to decrease surface load, specimens were coated with approximately 10 nm thickness Pt layer by a device for vacuum coating JEC-3000 FC of the Japanese company JEOL .

Electron microscopy morphological figures offer porous phase composition in our material, at various magnifications. Table 8 gives the results of pore analysis. Pores are mainly rounded, but if there are no such pores, latitudinal and longitudinal data of pores are taken and the average diametric result is calculated. Total volume of closed pores reaches 3.1 %. Through and half-through pores are not observed in the matix. According to morphological picture we can state that pore distribution in the material is between homogeneous and non-homogeneous. Therefore we considered that pore distribution factor in the matrix =0.9.

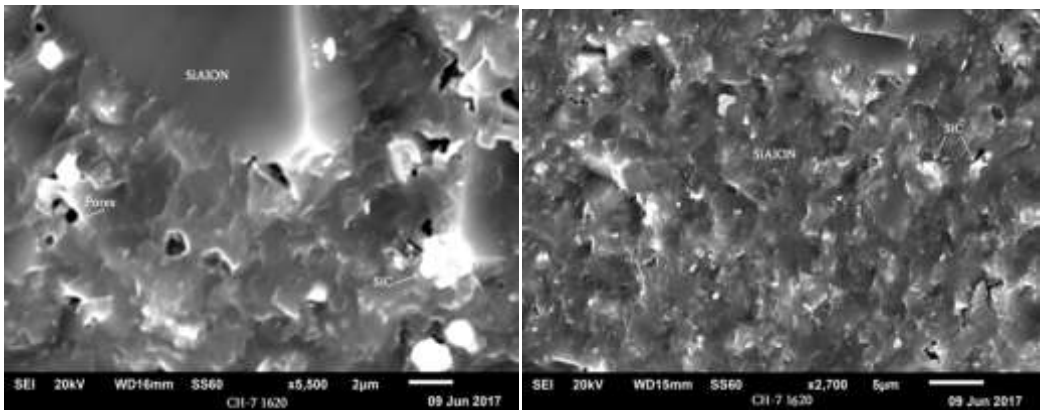

Fig. 13. Analysis of porous phase in hot-compressed CN 21 material

Table 8 Porous phase analysis

indentation picture #	vision area S, μM^2	number of counted pores, n	largest pores Dmax. μM	smallest pores Dmin. μM	average pores Dmid. μM	pores composition,%
27	1100	9	2.2	0.4	1.60	2.85
30	1600	18	2.8	0.8	1.90	2.35
average		27			1.75	3.10

Crystalline phase composition and average sizes

Results of crystalline phase analysis are given in Table 9, which shows that a rather big number of grains were counted of silicon carbide, as awell as SiAlON and aluminum oxide. It enables us to judge of compound elements of the crystalline phase of the matrix. SiAlON is approximately 57% of matrix, silicon carbide – approximately 27%, pores – approximately. 3 %. X-ray structural analysis fixed aluminum oxide reflexes, which probably were emitted mainly from the geopolymer; perhaps its small concentration was due to aluminum nano-powder, since nitrogen was not purified. We considered that its concentration was 6%. As to the glassy phase, perlite is completely glassy mass that undergoes melting at 1240^0C.

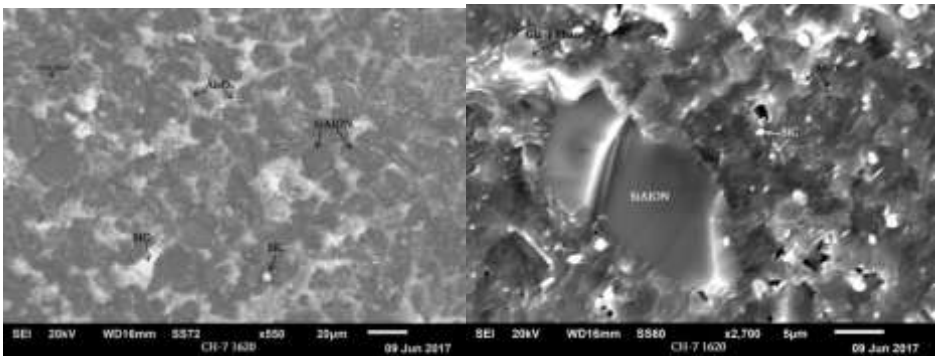

a) **b)**

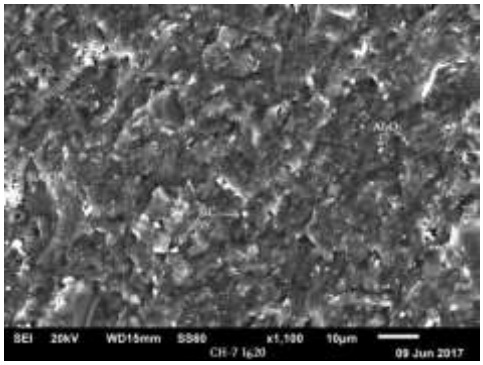

c)

Fig. 14 CN 21 a) , b), c) SiAlON crystalline phase composition and average sizes

Evidently 3% perlite added to the composite forms eutectic melts with geopolymer ingredients, especially with alkali oxides, which contributes to the increase of concentration of glassy phase in the material. We considered that its concentration equals to 7.4%.

Table 9 SiC, Al_2O_3 and SiAlON grain sizes and composition in matrix

indentation picture №	phase name	vision area S, μM^2	number of counted grains, n	largest grain Dmax., µM	smallest grain Dmin. µM	aver.grain Dmid. µM	phase composition, %
17	SiC	1740	85	33,05	2.70	4.80	26.8
13	SiC	3225	300	23.00	2.75	4.90	27.6
aver.						4.85	27.2
5	SIALON	35500	250	19.60	5.50	8.60	53.0
32	SIALON	8200	200	24.30	5.80	7.50	59.8
26	SIALON	1400	220	21.70	5.30	8.50	59.3
aver.						8.20	56.4
5	Al_2O_3	35500	60	2.6	1.27	1.93	5.7
grain average size, general						5.00	Kristal phase composition in matrix, general % 89.3

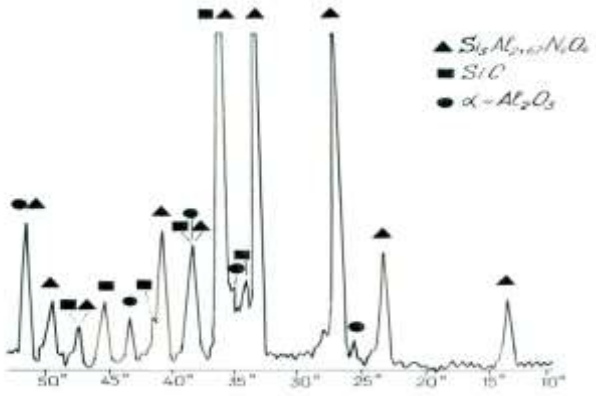

Fig. 15. CN 21 composite X-ray.

It is seen both from X-ray and electron-microscopy figures. Elasticity module, average, according to the Table 5 was defined - 145 MPa. Thus formula of Kovziridze's module, in numerical expression will acquire the following form:

$M=89.3x\ 145x\ 5.54x0.9\ /\ 5.0x\ 7.6x1.75x3.1=313\ MPa/\ \mu M^2$

As it was stated above this formula doesn't provide for Grifiths's defects [28] in the matrix, dislocations and other flaws in crystalline phases and nano-derangements in glassy phase. For the porcelain with 50% glassy phase, 25% mullite and 25% quartz crystalline phase, if we admit that elasticity module is approximately 75 MPa, Kic – 3.5, and porous phase data and crystals sizes are the same as in our tables, the value of the given module will equal to 8.7 Mpa/ μM^2. SiAlON ceramics is far stronger than the porcelain.

Electric properties of the material

Electric characteristics of the material obtained by hot compression are given in Table 10, while the resistance-temperature relation is given on diagram 16, where the studied material was marked by the index "A". The same table and diagram offer electric characteristics (marked by "B) of starting material obtained by nitro-alum thermal method; these data are taken from the reference [29].

Table 10 Effect of terms for material obtaining on its electric characteristics

specimen #	method of sample making	electric resistance at 298 K-, lgρ, λ•m	temperature coefficient of electric resistance, $a_T \cdot 10^{-2}$, K^{-1}	conductivity activation energy, E, ℓV
A	hot-compression	6.4	2.3	1.08
B	nitro-alum thermal synthesis	8.4	2.3	1.08

Relation "lgρ-T" is linear and for materials obtained by A and B versions are presented as parallel lines (Fig.16) ; besides, a_T and E values are identical, which refers to similar mechanism of current transfer (Table 10).

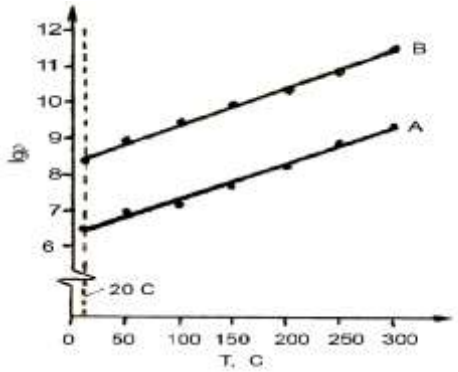

Fig.16. Changes in electric resistance in materials obtained by hot compression (A) and nitro-alum thermal synthesis (B) according to temperature.

Difference is fixed only in resistance values with the peculiarity that the hot-compressed sample "A" is characterized by 2 signs lower resistance than the material B, which was used to receive it. This should be associated with the transition of reactively baked structure of the hot-compressed material – to a dense, compact structure. Fig. 17 a and b shows the presence of bridging bridges between aluminum nanopowder grains by pearlite, which contributes to the improvement of mechanical properties.

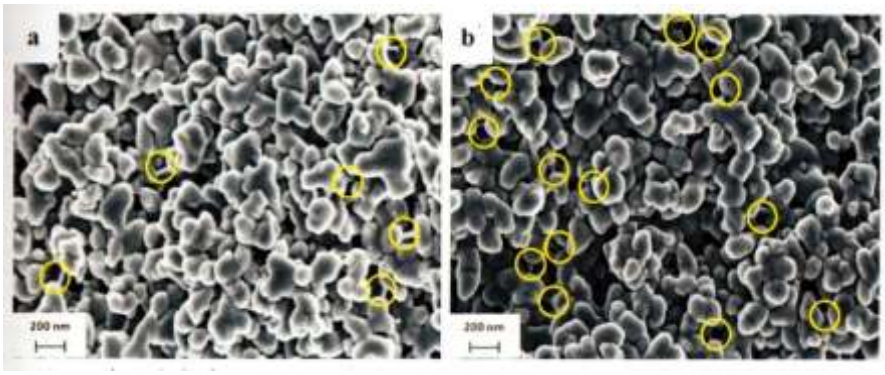

Fig. 17. The presence of connecting bridges between the grains of aluminum oxide in the matrix by glas pearlite.

3. CONCLUSION:

The composite was synthesized in the SiC-SiAlON-Al_2O_3 system by the method of reactive sintering using metal-thermal and nitriding processes. According to the results SiAlON's creation commences at 1200^0C and the process progresses intensely in the 1350-1450^0C range. Thus, we significantly reduced temperature of SiAlON synthesis; for reactive sintering – by approximately 550^0C and for hot-compression by approximately 130^0C, which was contributed greatly by glassy perlite additive. It is thanks to just formed imperfect crystalline lattice of silicon nitride, created at such low temperatures, which due to its relatively large hollow spaces receives alum oxide, aluminum nitride and silicon oxide. Then, at relatively high temperature, at1350-1450^0C it takes a form of ß- SiAlON structure. Mechanics at bending equals to 470 MPa, while at compaction 1910 MPa. Micro-mechanical analysis showed that in most cases a crack in the SiAlON matrix is not created and if it is created it is of small size. Similar result was observed at the interface of matrix-SiC grain. We computed the brittleness factor "B" of the material, which is not high. It shows low chances of swift spreading of a crack, while negative value of "n" factor refers to high hardness of the material to resist external mechanical loads at mechanical processing. The result was proved in the process of cutting specimens with diamond disks, when some disks were broken. High properties of the composite were confirmed when computing Kovziridze's mechanical module -313 MPa/ μM^2. The obtained results exceeded our expectations. The material was obtained through solid phase sintering. It is proved by relatively small concentration of glassy phase, which is less than 12%. Study of electric properties showed that a_T and E-values are identical, which refers to unalterability of a mechanism of current transmission (Table 9). Difference is fixed only in resistance values with the peculiarity that the hot-compressed specimen A is characterized with 2 signs lower resistance than the material B, which was used to receive this specimen. Probably such difference is conditioned by transition of porous material into compact structure.

REFERENCES

1) Shvedkov E.L., Kovensky I.I., Denisova E.T., Zyrin A.V. – Dictionary – Reference Book for new ceramics; Kiev, Naukova Dumka, 1991. p. 182.
2) Ekstrom T., Kall P.O., Nygren M., Olsson P.O. - Dense Single-Phase Beta-Sialon Ceramics by Glass-Encapsulated Hot Isostatic Pressing. –J .of mat. Sci.- 1989. V.24. p. 1853-1862.
3) Rosenflanz A., I-Wei-Chen.- Phase relationships and stability of a-SiALON,-J.Am.Ceram. Soc. 1999. V.82. №4. P. 25-28.
4) Strelov K.K. Theoretical bases in technology of refractory materials: handbook for high institutions/ K.K Strelov, I.D.Kashcheev, 2nd edition, revised; - M., 1996, pp. 608.
5) Chukhalina L.N. Method to obtain SiAlON powder http://bd.patent.su/2378000 last reviewed on- 18. 11.2012.
6) Zheng G, Zhao J., Gao Z., Cao Q., - Cutting performance and wear mechanisms at Sialon-Si_3N_4 graded nano-composite ceramic cutting tools/ The International Journal of advanced Manufacturing Technology, 2012 V.58 , I. 1-4. P. 19-28.
7) Tressler R. E. Theory and experiment in corrosion of advanced ceramics//Corrosion of Advanced Ceramics/ NATO ASI Series E: Applied Sciences/Ed. K.G.Nickel.-The Netherlands. 1994. #267. p. 3-22.
8) Piekarczyk J., Lis J., Bialoskorski J.- Elastic properties, hardness and indentation Fracture toughness of beta-Sialons/ Key Engineering Materials.- 1990. V. 89-91, p. 542-546.
9) Trigg M. B., Jack K.H. SiAlON Ceramics// J. Mat. Sci.- v.23. 1988. p. 481-487.

10) Jiang X., Baek Y. K., Lee S. M., Kang S.J.L.//Formation of an a – SiAlON layer on β – SiAlON and its effect on mechanical properties, J.Am. Ceram. Soc., 1998, v.81, № 7, p. 1907 – 1912.
11) Zhen-Kun H.// Formation of N-phase and phase relations in MgO-Si_2N_2O-Al_2O_3 system. J. Am. Ceram. Soc., v.77, p. 3251, 1994.
12) Lavrienko V.A. et al. High temperature oxidation of β-SiAlON powders in air flush//Refractories and technical ceramics. 2005. №2, p.8-11.
13) Phelps F. E.. Process for producing silicon aluminum oxynitride by carbothermic reaction/USA Pat. No. 4977113, C01B 033/26-№351660;/ Appl. on15.05.89. Published: 11.12.90.
14) Gauckler L.J., Beshovic S., Petrow G.- In books: Nitrogen Ceram. Proc.Nato Ady. Study Inst. Canderbury, 1976. Noordroff-Leyden, 1977, p. 405-414.
15) Yeh C. L., Sheng K. C., Effect of α-Si3N4 and AlN additional on formation of α-SiAlON by combustion synthesis / // Ibid. – 2011. – Vol. 509, iss. 2. – P. 529-534.
16) Cutler I. B.(USA)/ Process for producing a solid solution of aluminum oxide in silicon nitride/Pat.3960581 USA, C04D 035/58- №465222; Appl.29.04.74; Published.01.06.76; p. 16
17) Cho Y. W., Carles J.A., Synthesis of nitrogen ceramic powders by carbothermal reduction and nitridation. Part 2 Silicon aluminium oxynitride (sialon)/Mater. Sci.,1991. V.7 p.399.
18) Gavrish A. M., Puchkov A.B., Boyarina et al.,β-SiAlOn formation in the Si_3N_4-Al_2O_3-AlN system. Refractories, 1988, №8, p. 28-29.
19) Guzman I.Ya., Tumakova E.I., Fedotov A.V. Correlative study of some properties of materials based on composites SiC+Si_3N_4 и SiC – Si_2N_2, M.,Refractories, 1970, №3, p. 44-48.
20) Ogbuji L.U.J.T.- Role of Si_2N_2O in the passive-oxidation of chemically-vapor-deposited Si_3N_4,- J. Am. Ceram. Soc.- 1992, v.75-№11. P. 2995-3000.
21) Washburn M.E., Love R.W. A Silicon carbide refractory with a complex nitride bond containing silicon oxynitride// Am. Ceram. Soc. Bull. – V.41. – 1962.- #7. – p. 447-449.
22) Kovziridze Z.D. Development of scientific bases and technology of obtaining celsian and alumosilicate ceramic by the use of barite and perlite. Thesis for scientific degree of a doctor of technical sciences, Tbilisi, 1993. p. 41-50.
23) Kovziridze Z, Nizharadze N., Tabatadze D., Cheishvili T.,,Mestvirishvili Z., Nikoleishvili E., Mshvildadze M., Darakhvelidze N. Obtaining of nanocomposites in SiC-SiAlON and Al_2O_3-SiAlON system by alumothermal processes. Journal of Electronics Cooling and Thermal Control. 2014. 4. p.2-13.
24) B. Eftekhari Yekta1, Z. Hamnabard. Investigation of the mechanical properties and machinability of fluorphlogopite-gehlenite glass-ceramics. Journal of Ceramic Science and Technology. Vol.4 No. 4 2013. pp. 193-196. Baden-Baden. Germany. www.ceramic-science.com
25) Anstis, G.R., Chantikul, P., Lawn, B.R., Marshall, D.B. A critical evaluation of indentation techniques for measuring fracture toughness, direct crack measurements. J.Am. Ceram.Soc. 1981.vol. 64,No.9, p. 533.
26) **Journal of Georgian Ceramists Association "Ceramic and Advanced Technoligies" Vol. 19. 2(38), pp. 3-9. 2017 (in print. Will be published in December 2017) www.ceramics@gtu.ge**
27) **(National Center of Intellectual property of Georgia "Georgian Patent", Certificate of Deposition # 7136. "Formula of Mechanical Modulus of Ceramic Materials and Composites". 2017.10.11)**
28) Grifith A.A. Phil. Trans. Roy. Soc. London A221 1920.
29) Kovziridze Z., Nijaradze N., Tabatadze G,, Cheishvili T.,, Darakhvelidze N., Mestvirishvili Z., Mshvildadze M., Nikoleishvili E. Obtaining of SiAlONs by nitro-alum-thermal processes. J. of Association of Georgian Ceramists "Ceramics". # 2 (32), 2014, p. 23-31.